STUDY OF UNSTATIONARY PULSED AIR JETS FOR SORTING OPERATIONS

Thiago Ferreira, Sylvie Sesmat, Eric Bideaux, Fabien Sixdenier

Proceedings of the 9th JFPS International Symposium
on Fluid Power, Matsue, 2014
Oct. 28 - 31, 2014

1B2-4

STUDY OF UNSTATIONARY PULSED AIR JETS FOR SORTING OPERATIONS

Thiago FERREIRA*, Sylvie SESMAT, Eric BIDEAUX, Fabien SIXDENIER

Laboratoire Ampère, Université de Lyon
25, Avenue Jean Capelle, Bât. Leonard da Vinci
69621 - Villeurbanne, France
* (E-mail : thiago.caetano-ferreira@insa-lyon.fr)

ABSTRACT

Pulsed air jets are used in industries in order to perform sorting operations of different objects. Depending on the size and shape of the parts, the jet has different requirements. In this way, it is important to know the topography of the air jet and also its dynamic behavior during the pulse generation. This paper presents the results of measurements performed on subsonic pulsed air jets. It was possible to notice that, even on pulse generation, the jet presents the same topography as the one of steady state jet. Thus, it respects the analytical expressions found in the literature. The different delays related to the spatial propagation along the axis of the jet were also observed. Moreover, the results evidence the decrease of the jet quantities at operation frequency of 80 Hz where velocities magnitude was not able to reach the nominal values when compared to the tests performed at 10 Hz. The tests inside the potential core show a good repeatability of the jet quantities even outside the x-axis. This zone of high pneumatic energy is a good candidate in order to perform sorting applications. Further work consists on evaluating different valves, nozzle diameters, and chambers between them in order to identify which parameter can be optimized in order to have a fast and effective jet for ejection.

KEY WORDS

Air jet, Sorting, Fast switching valve

NOMENCLATURE

C_m	:	*flow parameter*
d	:	*diameter*
f	:	*frequency*
M	:	*Mach number*
p	:	*pressure*
R	:	*gas constant*
T	:	*temperature*
t	:	*time*
u	:	*velocity in x direction*
V_{mag}	:	*velocity magnitude*
x	:	*position along x-axis*
y	:	*position along y-axis*
z	:	*position along z-axis*
γ	:	*ratio of specific heat*
ρ	:	*density*

Exponents and indices

0f	:	*fictive length of potential core*
atm	:	*atmospheric*
m	:	*in the axis of the jet*
N	:	*Nozzle*
res	:	*reservoir*
up	:	*upstream*

INTRODUCTION

Sorting operations using pulsed air jets are widely used in industries nowadays for food, minerals and waste processing. However, the manipulation of different objects, such as a single rice grain or a silver nugget, can be considered as distinct operations in terms of jet specifications. For instance, to eject rice the jet must be narrow and precise, due to the rice's size and shape. Nevertheless, for the nugget, the jet must have a bigger cross section. This will ensure the ejection force to be applied over a bigger surface to expel the object and not only induce a rotation. At the same time, the pneumatic energy needed to eject an object depends on the speed, trajectory and mostly the weight of the part to be ejected.
As can be noticed, in order to perform a sorting operation it is important to know the topography of the air jet and identify the shape and different zones in which the ejection can be successfully executed. At the same time, the pulsed air jet can be generated at different frequencies. Due to this fact, the dynamic behavior of the jet during its expansion must also be known.

CONTEXT

In the past few years, the industry and the scientific community have been working on system capable to perform sorting operations. Most of these studies are being carried on the development and optimization of solenoid valves in order to shorten the mechanical response time and to decrease the pressure drop on the fluid flow while crossing this element. However, the air jet must also be studied in order to perform an efficient ejection.
Although the stationary behavior of the air jet in different conditions is analytically described [1-2] and experimentally characterized [3], the dynamic behavior of the generated pulsed air jets remains yet to be determined. This study may lead to a better understanding of the jet generation, which could help the design of more efficient components and possibly decrease air consumption.
To study the development of these pulsed air jets a test bench has been developed [4] and the first results for stationary conditions for subsonic and supersonic air jets were presented in [3].
Thereby, different tests must be performed in order to validate the experimental procedure for the measurements of jets' dynamics. This paper presents the experimental results for subsonic air jet.

Structure of a subsonic air jet

Inside a stationary subsonic air jet (Figure 1) three different zones can be distinguished:

-Potential core (red): cone shaped region where pressure, velocity and temperature are not affected by gravity;
-Mixing zone (purple): region where the air jet interacts with the surrounding atmosphere;
-Fully expanded zone (not represented): region where the gravity forces are preponderant and the jet quantities decrease until they are mixed with the atmosphere.

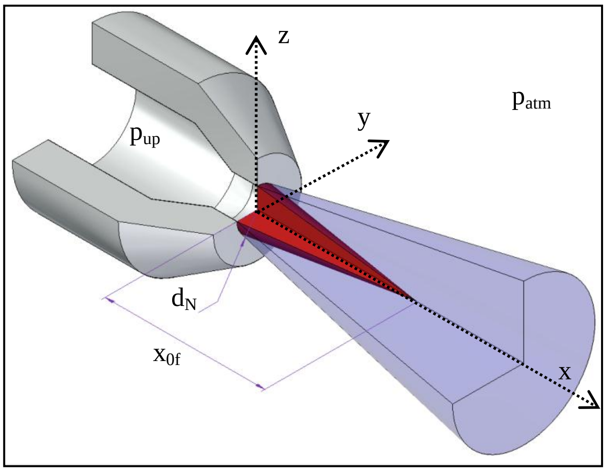

Figure 1 Representation of a 3D air jet

This stationary topology was experimentally validated [3], but in sorting operation it is also important to understand how the jet reaches these stationary conditions.

OBJECTIVE

This paper presents the experimental dynamic characterization of the flow circuit from the valve up to the jet during pulse generation. The results enable the understanding of the dynamic establishment of the jets and help to identify its transitory behavior when switching the solenoid valve on and off.
The results can also help the determination of the limit operational frequency at which the jet no longer reaches its required energy to perform the ejection of different objects for a given solenoid valve.

EXPERIMENTAL PROCEDURE

Generating the air jet

The valve used in this experimental procedure is an electro-pneumatic solenoid valve. The first stage is composed by an electromagnetic actuator while the main stage is a spool and sleeve actuator. Once the first stage is set ON, the air can flow from the upstream

chamber through a secondary channel and push over the spool of the valve's main stage. The spool starts to move when the pressure is high enough to overpass the force of the return spring in the second stage.
When the solenoid valve is opened, the air can flow from the upstream chamber across the valve and reach the nozzle at outlet of the system (Figure 2).

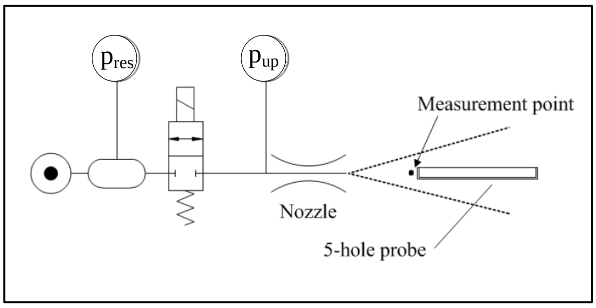

Figure 2 System's scheme

Exploring the jet

In order to explore the dynamic behavior of the jet, the experimental test bench developed and detailed in [4] is used. This system allows the measurement of different physical phenomena along the circuit generating the jet (pressures, temperature, as well as the drive signal and spool displacement).
A 5-hole probe (Figure 3 on top) mounted on a 3-axes robot gives the information of temperature and 5 different pressures measured at its tip. By using the calibration tables and reconstruction procedure [5-6], it is possible to calculate the velocity magnitude, Mach number, total and static pressures and temperatures at different points inside stationary or unstationary jets (Figure 3 on the bottom).
In order to minimize the disturbance of the probe on the air jet, the probe dimensions must be reduced. In this miniaturization process the 5 pressure sensors embedded on the probe are deported. Thus, small pneumatic tubes are placed in the probe's nose to allow the measurement of the pressure value at its tip (Figure 4 on top).
For tests performed under stationary conditions, this deportation has no influence on the measured values. However, for the transitory phenomena, the presence of these tubes causes an attenuation of the pressure magnitude and also inserts a delay on the measured values.
The signal measured (b(t) in the Figure 4) is a deformation of the pressure at the measurement point (a(t)). Thus, the signals must be corrected [7-8].
In order to do this procedure, the identification of the attenuation and delay for the 5 tubes was performed by the probe manufacturer using reference sinusoidal signals with frequencies up to 1,6 kHz.

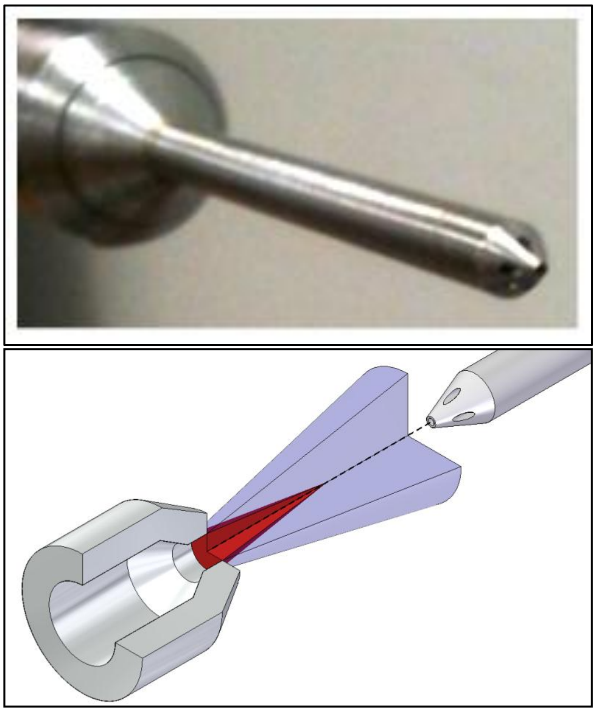

Figure 3 5-hole probe's tip

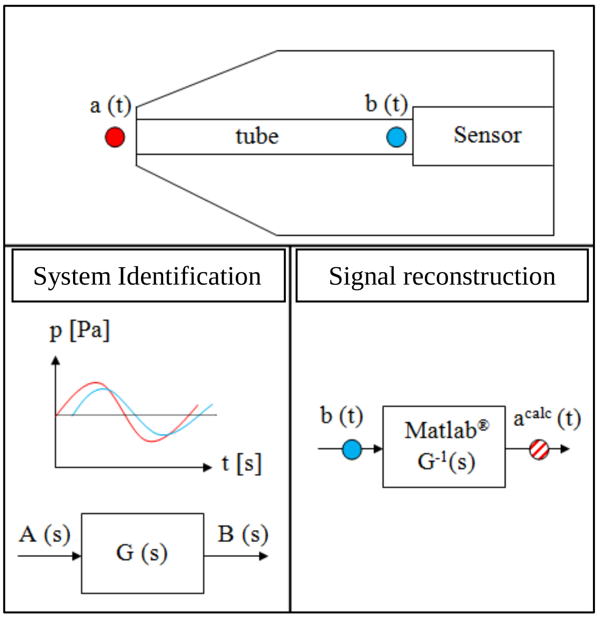

Figure 4 Reconstruction procedure of pressure signals

The values of attenuation and delay where used to identify the transfer function G(s) of each one of the 5 tubes.
By using Matlab®, the signal $a^{calc}(t)$ (estimation of real value a(t)), can be calculated by using the inverse transfer function of the system $G^{-1}(s)$.
This procedure allows the correct measurements of physical quantities of the jet during dynamic operations. Therefore, the measurements are performed with the valve driven by a square input signal at different frequencies with nozzle having a diameter d_N= 3 mm. The sampling frequency of the acquisition system is 10 kHz per channel, in this way, the measurement uncertainty on time is 0.05 ms. In order to avoid data losses all the data are processed offline.

Pulsed air jets along the axis
The steady state behavior of an air jet is already known. However, one of the main questions about the pulsed air jets is if it still reaches the quantities of a steady state air jet in the same upstream configuration.

Theory Vs Measurement
In subsonic stationary conditions the velocity magnitude along the x-axis was analytically described in [1]. Inside the potential core ($x<x_{0f}$ as represented in Figure 1), the velocity magnitude remains constant and has in theory the same value of the velocity magnitude at the nozzle, u_N . The velocity $u_m(x)$ along the x axis of the jet can be calculated by Eq. (1).

$$u_m(x)=\begin{cases} u_N \cdot \left(\frac{x_{0f}}{x}\right)^{1.125}, & \text{for } x > x_{0f} \\ u_N, & \text{for } x<x_{0f} \end{cases} \quad (1)$$

Where:

$$x_{0f}=4.7 \cdot d_N \cdot \left(\frac{p_{up}}{p_{atm}}\right)^{0.42} \quad (2)$$

Considering the flow in an ideal convergent nozzle [9], the value of u_N can be calculated by Eq. (3).

$$u_N=\frac{p_{up}}{\rho_{up}\sqrt{T_{up}}}C_m \quad (3)$$

For subsonic conditions the flow parameter C_m is described by Eq. (4):

$$C_m=\sqrt{\frac{\gamma}{R}\left\{M_{up}^2\left(\frac{p_{atm}}{p_{up}}\right)^{\frac{2}{\gamma}}+\frac{2}{\gamma-1}\left[\left(\frac{p_{atm}}{p_{up}}\right)^{\frac{2}{\gamma}}-\left(\frac{p_{atm}}{p_{up}}\right)^{\frac{\gamma+1}{\gamma}}\right]\right\}} \quad (4)$$

In order to evaluate the velocity magnitude along the x-axis, the 5-hole probe is placed inside the jet at different x positions. The tests were performed in the conditions presented in Table 1.

Table 1 Conditions of the dynamic tests along x-axis

p_{atm}[Pa]	101800
T_{atm}[K]	291.63
x positions [mm]	4, 9, 14, 19, 24, 34, 44, 64, 84, 104
Frequency [Hz]	10
p_{res} [Pa]	508000
p_{up} [Pa] (steady flow)	154500
T_{up}[K]	294.65

Figure 5 presents the measured values of velocity magnitude during one air pulse for different x positions.

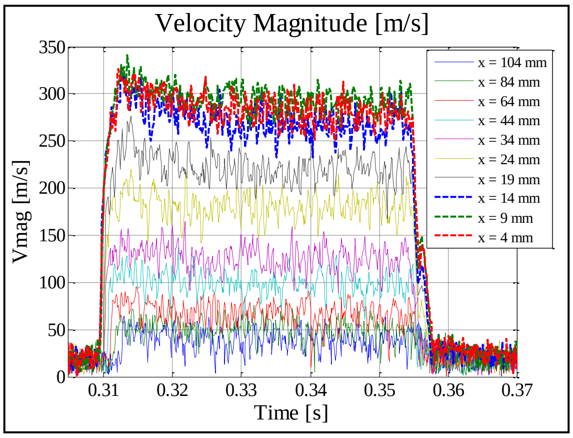

Figure 5 Velocities magnitude for pulse generation at f=10Hz in different x positions.

As can be noticed, the velocities at the points x = 4, 9 and 14 mm (dotted lines) have similar average velocity magnitude, which corresponds to the potential core of a subsonic air jet. Moving further in the same x-axis, the velocities values start to decrease.
The average values of velocity magnitude measured in the different positions are presented in Figure 6 and compared to the theoretical values (Eq. (1)) for the conditions presented in Table (1).

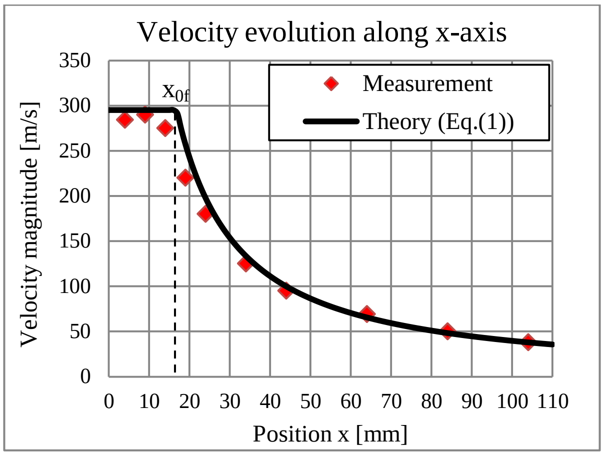

Figure 6 Comparison between the analytical curve and experimental results

Inside the potential core ($x<x_{0f}$) the measured values of velocity $u_m(x)$ are lower than the theoretical values. This was expected, due to the fact that in a real flow there are pressure drops along the circuit.

As the upstream pressure p_{up} is measured 16 mm upstream the nozzle outlet, the pressure generating the air jet can be slightly lower than the measured value. Despite this small discrepancy in the potential core, the measurements evolve with the same shape as the theoretical values.

It can also be noticed that the velocities around the x_{0f} position are lower than expected. This was also observed by Leonhard [1]. Due to this fact x_{0f} is called the fictive length of the potential core. In the reality the velocities inside the potential core starts to decrease at the position x_0 (real length of the potential core) with $x_0 \leq x_{0f}$ and depends on the conditions generating the jet.

For this test, the working frequency was set to 10Hz and during each pulse the jet had enough time to reach a steady state behavior. However, different tests were also performed at higher frequencies and the repeatability and propagation time were evaluated.

Tests at higher frequencies

The tests performed at different frequencies presented very similar results. For this reason, in the following session, the jet's dynamics measurements along the x-axis will be presented only in the case of a working frequency of 80 Hz. Table 2 presents test conditions.

Figure 7 presents, on top, the pressure p_{up} during pulse generation. At a first glance it is possible to notice a similar behavior from one pulse to another at different positions. Moreover, the rising edges of the p_{up} have a good repeatability and a small dispersion in time, as can be seen in the detail of upstream pressure between 0.557 and 0.563 seconds (second figure from the top).

Table 2 Conditions of the dynamic tests, f = 80 Hz along x-axis.

p_{atm}[Pa]	101490
T_{atm}[K]	297.35
x positions [mm]	4, 6.4, 9, 11.5, 14, 16.5, 19, 24, 34
Frequency [Hz]	80
p_{res} [Pa]	504000
Max p_{up}[Pa]	166500
T_{up}[K]	294.5

This fact evidences the repeatability of the valve on generating the jet even at high frequencies.

During the same time window, the rise of the total pressure in the different measurement points can also be analyzed (third figure from the top). As can be seen in this figure, the total pressure at point x = 4 mm (closest to the nozzle) starts to rise after a small delay following the total upstream pressure p_{up}. As we move further along the x-axis, this delay is increased.

At the same time, the maximum values of total pressure and velocity decrease along the axis, except for the points inside the potential core (dotted lines) where the values remain the same, but are also affected by time delay which depends on the x position. This behavior was also observed in the tests performed at f = 10 Hz (Figure 5).

However, even if the upstream pressure has still a good repeatability even at 80 Hz and presents a similar behavior as the tests at lower frequencies, the pulses here do not reach the same total pressure and velocity values inside the air jet.

The upstream pressure reaches values of 166500 Pa during a short time, but inside the jet the total pressure rises until a maximum value of 149000 Pa. Figure 7 on bottom presents the velocity magnitude, and it is possible to see that the values inside the potential core do not have enough time to reach and stabilize at their maximum values. The duration of the pulse is limited and the values start to decrease.

This test was performed at similar conditions as the tests at operation frequency of 10 Hz in which the velocities have reached values around 300 m/s inside the potential core (Figure 5). Here, the velocities in the same zone have reached values of 250 m/s. Therefore, the pulse generated at the same conditions for f = 80 Hz does not have the same pneumatic energy as the jet for f = 10 Hz, which can affect the ejection operation.

These results evidence the dependency of the jet quantities on the operation frequency.

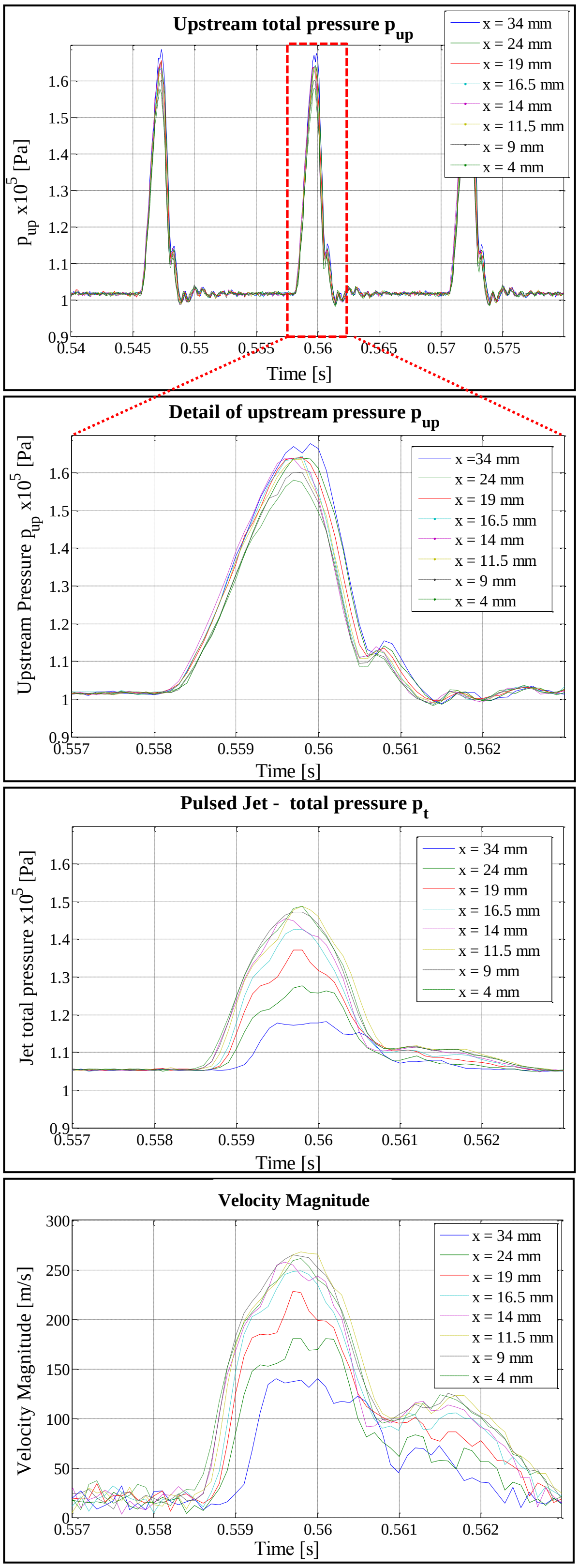

Figure 7 Jet characteristics for f = 80 Hz.

Dynamic behavior inside the potential core

A first measurement of dynamic establishment of the air jet was performed along the jet's axis. It was possible to see the repeatability of the air quantities in the center line of this core.

However, to perform the ejection, these quantities must be repeatable over a surface in order to have enough energy to deviate the object.

In this section, the behavior of the air jet in different planes perpendicular to the x-axis is evaluated for different x positions as represented in Figure 8.

As the air jet is axisymmetric the measurements are presented for points along the y-axis (see Figure 1).

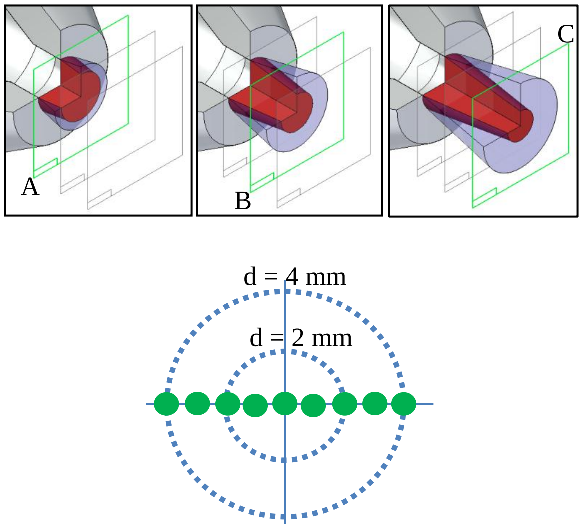

Figure 8 Representation of the measurements planes and points.

Table 3 presents the parameters of the dynamic tests for 3 planes perpendicular to the jet's axis.

Table 3 Conditions of the dynamic tests on different planes

p_{atm}[Pa]	101500
T_{atm}[K]	296.85
x positions [mm]	A: 9; B: 11,5; C: 14
Frequency [Hz]	60 Hz
p_{res} [Pa]	502000
Max p_{up}[Pa]	163500
T_{up}[K]	294.15

Figure 9 presents the velocities measured in the plane A. The center point is placed in the x-axis and inside the potential core. The red, purple, green and black lines have the similar velocity magnitude as the measurement in center of the plane, which indicates we are still in the potential core (red circle at the figures). However for the dark blue and mustard points the velocity magnitude is lower than the other. These points are placed inside the mixing zone.

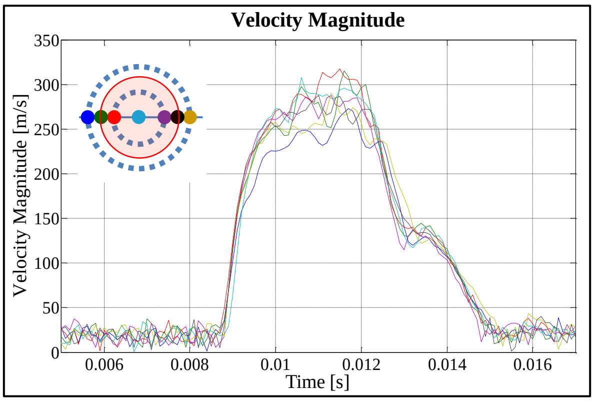

Figure 9 Measurements in the plane A at x = 9 mm.

For the plane B, the measurements were performed at the same points. In this case, it is clear to notice in Figure 10 that the dark blue, green, black and mustard are completely outside the potential core as their velocity values are lower than the measurements in the center points. The red and purple are placed in the limits of the potential core.

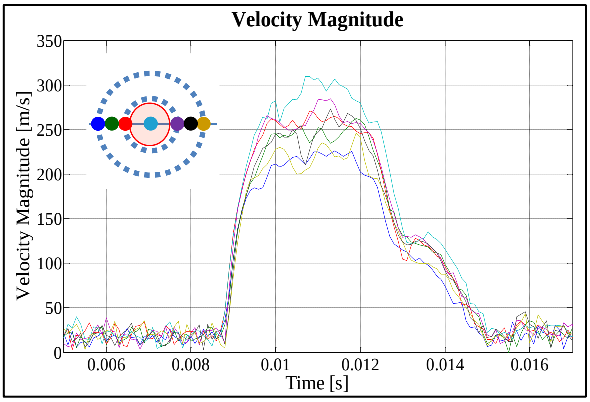

Figure 10 Measurements in the plane B at x = 11.5 mm.

Moreover, at the plane C (Figure 11), as the measurements are performed at x = 14 mm, the potential core is ending. Thus, intermediate measurements points are used in order to identity the limits of the potential core.

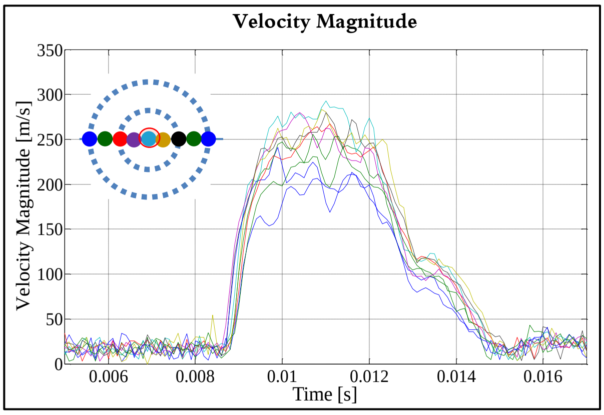

Figure 11 Measurements in the plane C at x = 14 mm.

Except the blue curve in the center, the measurements in the other points have a lower velocity magnitude. The purple and mustard points are placed inside the transition place between the potential core and the mixing zone. The other curves are outside the potential core. It can be notice as well that in plane C the rising of the velocity magnitude have a bigger dispersion as we leave the core zone.

Figure 12 presents the measurement inside the potential core at the different planes. It is possible to notice that inside the potential core, in addition to have the same velocity, the dynamic behavior has a good repeatability. Moreover, this zone with high pneumatic energy is a good candidate to perform ejection operations as the jet quantities are at their maximum values in the jet.

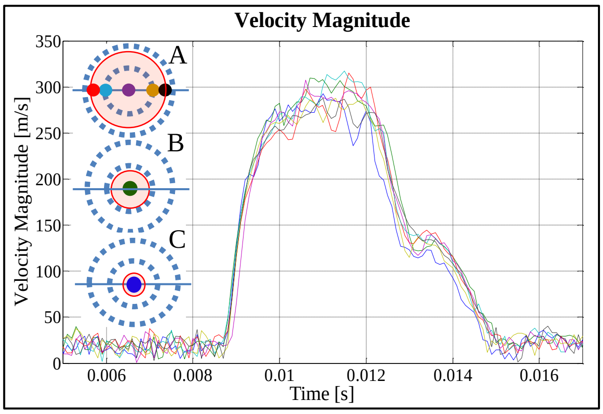

Figure 12 Measurements inside the potential core at different planes

CONCLUSIONS AND PERSPECTIVES

This experimental study of pulsed air jet generation gives a better understanding of the jet's dynamics. It was possible to notice that for low frequencies such as 10 Hz, the jet has enough time to settle to the steady state values along its axis described in the literature. However, for tests at higher operation frequencies (80 Hz), even if the upstream pressure generating the jet having a similar behavior as for tests at low frequency, the jet was not able to reach its maximum values. The dynamic tests performed inside the potential core of pulsed air jets (not only in the center line of the jet) show a good repeatability of the rising velocity magnitude. This zone of high pneumatic energy is a good candidate in order to perform sorting applications. Further work consists on performing measurements at the subsonic potential core of supersonic air jets. Moreover, the evaluation of different valves, nozzle diameter, and chamber between them, will be also realized in order to identify which parameter can be optimized in order to have a fast and effective jet for ejection.

ACKNOWLEDGMENTS

The authors thank the students Audrey Dubus, and Virgile Velletaz for their help in performing the tests.

REFERENCES

1. Leonhard, A., Untersuchungen zum pneumatischen Sortieren von Schüttgütern mittels Freistrahlen. PhD Thesis. Dresden. 2010
2. Dubois, J., Etude expérimentale de jets libres compressibles ou en présence d'un obstacle. PhD Thesis. Marseille. 2010
3. Ferreira, T., Sesmat, S., Bideaux, E., Sixdenier, F., Experimental analysis of air jets for sorting applications. Proceedings of the 8Th FPNI Ph.D Symposium on Fluid Power. Lappeenranta, 2014.
4. Ferreira, T., Sesmat, S., Bideaux, E., Sixdenier, F., Fast switching pneumatic valves: experimental bench for flow and pulsed air jet characterizations. 13th Scandinavian International Conference on Fluid Power, June 3-5, Linköping, 2013
5. Truong, S.S., Conical Probe Calibration and Wind Tunnel Data Analysis of the Channeled Centerbody Inlet Experiment. Bachelor Thesis. California Polytechnic State University. 2011
6. Johansen, E.S., Rediniotis, O.K., Jones, G., The Compressible Calibration of Miniature Multi-Hole Probes. Transactions of the ASME. Vol 123. 128-137. 2001.
7. Telionis, D., Yang, Y., Rediniotis, O., Recent Developments in Multi-Hole Probe (MHP) Technology. Proceedings of 20th International Congress of Mechanical Engineering. Brazil, 2009.
8. Carvin, C., Consigny, H., A practical data reduction procedure to account for the response time of pressure measuring systems. 70th Semi-annual STA Meeting. England. 1988
9. White, F., Fluid Mechanics. 4th edition. Chapter 9. 2002